CALCUL DES VIBRATIONS AVEC IMPACT ET FROTTEMENT D'UNE STRUCTURE TUBULAIRE AVEC SUPPORTS A JEUX

COMPUTATION OF IMPACT-FRICTION INTERACTION BETWEEN A VIBRATING TUBE AND ITS LOOSE SUPPORTS

EDF
Electricité de France

Direction des Etudes et Recherches

Service Information Prospective et Normalisation

CLAMART Le 04/10/94

Département Systèmes d'information et de documentation

Groupe Exploitation de la Documentation Automatisée

1, avenue du Gal de Gaulle
92141 CLAMART Cedex
tel : 47 65 56 33

BAT 526
CEN SACLAY
MIST/SBDS/SPRI
MIST-SDEM-SBI

91191 GIF SUR YVETTE CEDEX

à l'attention de :

MEMOIRE TECHNIQUE ELECTRONIQUE

****
Cette feuille est détachable grâce à la microperforation sur le coté droit.
****

Référence de la demande : **F486735** Votre commande :
Origine : **AVIS DE PARUTION NORMES E**

Numéro du document : **94NB00040**

Titre : **CALCUL DES VIBRATIONS AVEC IMPACT ET FROTTEMENT D'UNE STRUCTUR TUBULAIRE AVEC SUPPORTS A JEUX**

Auteurs : **JACQUART G./GAY N.**

Source : **COLL. NOTES INTERNES DER. PRODUCTION D'ENERGIE (HYDRAULIQUE, THE**
Serial :

Référence du document : **SANS**

Nombre de pages: **0019** Nombre d'exemplaires : **001** Support : **P**

EDF
Electricité de France

Direction des Etudes et Recherches

SERVICE RÉACTEURS NUCLÉAIRES ET ECHANGEURS
Département Transferts Thermiques et Aérodynamique

SERVICE ENSEMBLES DE PRODUCTION
Département Acoustique et Mécanique Vibratoire

1993

JACQUART G.
GAY N.

CALCUL DES VIBRATIONS AVEC IMPACT ET FROTTEMENT D'UNE STRUCTURE TUBULAIRE AVEC SUPPORTS A JEUX

COMPUTATION OF IMPACT-FRICTION INTERACTION BETWEEN A VIBRATING TUBE AND ITS LOOSE SUPPORTS

Pages : 19

94NB00040

Diffusion : J.-M. Lecœuvre
EDF-DER
Service IPN. Département SID
1, avenue du Général-de-Gaulle
92141 Clamart Cedex

ISSN 1161-0611

SYNTHÈSE :

Le maintien des composants des PWR en état de fonctionnement fiable exige des travaux complexes de conception pour prévenir différents processus d'endommagement notamment les vibrations provenant des écoulements et les mécanismes d'usure. Pour améliorer la prédiction des interactions tube/support et de l'usure des composants des REP, EDF a entrepris un vaste programme comportant à la fois calculs et expériences.

Cette note décrit le développement numérique réalisé par EDF à l'aide du code informatique de calcul mécanique Aster afin de calculer la dynamique non linéaire des structures tubulaires avec des supports à jeux. Des validations numériques et expérimentales de ce code sont également données.

La technique numérique de la simulation dynamique repose sur une méthode de décomposition de Ritz, qui comporte une méthode de superposition modale semblable à celle employée dans d'autres codes informatiques. L'expression explicite des forces d'impact et de frottement permet d'utiliser un schéma d'intégration explicite rapide. Différentes bases de projection sont comparées. Certaines sont capables d'améliorer de façon significative la résolution du problème dynamique.

La validation numérique du code consiste en des simulations de certaines configurations mécaniques (analytiques ou calculées) trouvées dans la littérature. La comparaison des résultats des calculs avec les données disponibles dans la littérature révèle la haute précision du code informatique.

Une validation de certaines données expérimentales est aussi fournie. L'expérience ayant servi à cette validation consiste en un tube en U à supports multiples, avec quatre supports à jeux dans la courbure du U, et soumis à des forces d'excitation harmoniques et à bande large. Trois d'entre eux correspondent à des jeux faibles Gs et le quatrième à un grand jeu G1 (G1=15Gs). Dans cette expérience, on fait varier les forces d'excitation. Pour chaque configuration, la réaction du tube est calculée et comparée aux résultats expérimentaux. L'analyse des paramètres régissant l'usure conclut à une bonne conformité entre les valeurs calculées et les valeurs mesurées.

EXECUTIVE SUMMARY :

Maintaining PWR components in reliable operating condition requires complex design to prevent various damaging processes including flow-induced vibration and wear mechanisms. To improve prediction of tube/support interaction and wear in PWR components, EDF has undertaken a comprehensive program involving both calculations and experiments.

This paper describes EDF numerical development with the Aster mechanics computer code to calculate the non-linear dynamics of tubular structures with loose supports. Both numerical and experimental validations of this computer code are given.

The numerical technique for dynamic simulation is based on a Ritz decomposition method, including the modal superposition method as used in some other computer codes. The explicit expression of impact and friction forces allows a fast, explicit integration scheme to be used. Different projection bases are compared. Some can improve significantly the resolution of the dynamic problem.

The code numerical validations consist in simulations of some mechanical configurations (analytical or computed) provided in the literature. The comparison of the Aster calculation results with the available data of the literature shows the high accuracy of the computer code.

A validation on some experimental data is also provided. The experiment used for this validation consists in a multi-supported U-tube, with four loose supports in the U-bend and submitted to harmonic and broad band excitation forces. Three of them correspond to a small gap G_s, and the fourth one to a large gap G_1 ($G_1=15G_s$). In this experiment, the excitation forces are varied. For each configuration, the tube response is computed and compared to the experimental results. The analysis of the parameters governing wear concludes to a good accordance between the calculated and measured values.

COMPUTATION OF IMPACT-FRICTION INTERACTION BETWEEN A VIBRATING TUBE AND ITS LOOSE SUPPORTS

G.Jacquart* and N.Gay**

Electricité de France (EDF)
Direction des Etudes et Recherches (DER), Clamart , Chatou***
France

NOMENCLATURE

M, K, C	mass, stiffness, damping matrices of a dynamic system
$R(t)$	external force vector
$G(X, \dot{X})$	non linear force vector
$[\Phi]$	system eigenmodes
ω	circular frequency
q	modal or generalized coordinates
$q, \dot{q}, \ddot{q}$	generalized displacements, speeds, accelerations
m_i, k_i	modal mass and stiffness of mode i
ω_i	eigen circular frequency
$[\Psi]$	static modes or constraint modes
d_n	normal distance to support
f_n	normal reaction force due to support
K_n	normal impact stiffness
C_n	normal impact damping
d_t	tangential position to support
f_t	tangential reaction force due to support
K_t	tangential adherence stiffness
C_t	tangential adherence damping
μ	Coulomb's sliding coefficient
δ_{ij}	Kronecker's symbol

I - INTRODUCTION

For some components of pressurized water reactors (PWRs), wear analysis has become a major concern for EDF, in view of the need to improve the life-time and upkeep of such components to maintain highly reliable generating conditions. Both steam generator tubes and control rods are examples of long, thin tubular systems, held or guided by loose supports. These components are subjected to flow-induced vibrations which lead to impact and friction on the supports. Wear resulting from the friction against supports now appears to be the most damaging phenomenon for those components. An comprehensive major program has been begun by the EDF Research and Development Division (DER) to determine or quantify possible flow excitation mechanisms for these components, to develop numerical simulation algorithms for impact/friction vibration, and, finally, to analyze wear mechanisms. The purpose of this program is to make it possible to predict the life-time of components and to devise structural modifications. A specific algorithm, including impact and friction, has been developed in the DER structural computer code Aster. This article describes the numerical method employed, shows some numerical examples compared with literature references, and compares experimental results in an industrial situation with numerical predictions. The algorithm selected to integrate the dynamic equations of the system is called a Ritz reduction method and is detailed in Section II. This strategy makes it possible to use the very common modal superposition technique as in many computer codes, for instance in Vibic [1] or in Gerboise [2]. Others projection base choices are also possible with this method and may eventually improve the results, these are described in Section III. The computed expressions of impact and friction forces developed between the tube and the support are described in Section IV. The reduced dynamic system is integrated by an explicit modified Euler scheme which is described in Section V. In Section VI, some numerical examples from the literature are treated and results are compared with others works. Finally, Section VII provides a relative comparison between numerical simulation and experimental measurements on a shaker test facility composed of a curved U-bend steam generator tube with four anti-vibration bars.

II - RITZ REDUCTION METHOD

A finite element representation of the dynamic equations of motion of a structure, leads to a differential problem formulated in matrix form as:

$$\text{find } X, \dot{X} \in R^N \;/\quad M.\ddot{X} + C.\dot{X} + K.X = R(t) + G(X, \dot{X}) \qquad (1)$$
$$\text{with } \quad X(t=0) = X^0 \,, \dot{X}(t=0) = \dot{X}^0$$

Some algorithms can solve directly Problem (1) using an implicit integration scheme like H3DMAP [3]. Unfortunately, they are usually rather slow because dealing with a large number of equations N. If the problem happens to be non-linear, those algorithms need iterations to find the equilibrium for non-linear forces and are therefore very time-consuming.

The RITZ reduction method consists in solving Problem (1) after its projection on a sub-space ϑ generated by a base of p vectors of R^N : $V = [v_1, v_2, ..., v_p]$. V is called the projection base. The reduced problem can then be written as :

$$\text{find } q, \dot{q} \in R^N \;/\quad V^t.M.V.\ddot{q} + V^t.C.V.\dot{q} + V^t.K.V.q = V^t.(R(t) + G(V.q, V.\dot{q})) \qquad (2)$$

$$\text{where, } \; q(t=0) = q^0 \,, \; \dot{q}(t=0) = \dot{q}^0$$

The approximate solution of Problem (1) is then given by the relation:

$$\tilde{X}(t) = V.\, q(t) \tag{3}$$

Vector q is the generalized displacements vector, containing components of displacement X according to vectors V. The accuracy of the approximate solution obtained for the reduced problem (2) compared with the exact solution of (1) is based on a judicious choice of V (number and form of base vectors). The evident benefit of this method is the gain in system size (N/p) which is usually considerable and thus reduces considerably the computing time.

The algorithm developed in the Aster structural computer code solves Problem (2) without any hypotheses or restrictions relating to the nature of Aster projection base V. Some particular bases suitable for the projection of a dynamic problem are now examined.

III - PROJECTION BASES

III.1 - Projection bases for a linear structure (omit $G(X, \dot{X})$ in (1))

III.1.1 - The modal base : A very common projection base used for a linear structure is the base of the first p eigenmodes of the linear undamped structure :

$$V = \Phi = [\varphi_1, \varphi_2, \ldots, \varphi_p] \quad / \quad \forall i\,, \exists\, \omega_i\,, \quad K.\, \varphi_i - \omega_i^2 M.\, \varphi_i = 0 \tag{4}$$

A first advantage of this projection choice is that the projected mass and stiffness matrices are diagonal (a characteristic of normal modes):

$$\varphi_i^t.\, M.\, \varphi_j = m_i\, \delta_{ij} \qquad \varphi_i^t.\, K\,.\, \varphi_j = k_i\, \delta_{ij}$$

This property improves some explicit numerical integration schemes for whose an inversion of matrix M projection is necessary. A second positive point of the modal base is that error E due to solving the projected problem (2) instead of the initial problem (1) can easily be written (in Fourier transform) :

$$E(\omega) = \sum_{i=p+1}^{N} \frac{\varphi_i.\, \varphi_i^t.\, R(\omega)}{-\omega^2\, m_i + k_i} \tag{5}$$

If the external forces R are characterized by a cut-off frequency at f_{max} (corresponding circular frequency : ω_{max}), we can derive from Equation (5) a clear strategy for determining the size of the modal base, which is to take the first p modes such that:

$$\omega_{p+1} \geq \alpha.\, \omega_{max} \quad \text{with} \quad \alpha = \sqrt{2} \tag{6a}$$

$$\left\| K^{-1}.\, R - \sum_{i=1}^{p} \frac{\varphi_i.\, \varphi_i^t.\, R}{k_i} \right\| \leq \beta.\, \|K^{-1}.\, R\| \quad \text{with} \quad \beta = 1\% \tag{6b}$$

The left term of Equation (6b) represents the residual flexibility of the structure to the external load, that is the flexibility not represented by the projection on the first p modes.

As an example, for a pinned beam we can show that the residual flexibility given by a mode p is inversely proportional to p^4 ; so the convergence of the flexibility is in that case relatively rapidly achieved. For compression modes, the flexibility of mode p is inversely proportional to p^2 and in that case the convergence of the flexibility is relatively slow.

The 'MacNeal projection base' described in the next Section is thought to improve the modal base for the representation of structural flexibility.

III.1.2 - MacNeal projection base : Assume that the external loading of Problem (1) can be written as:

$$R(t) = \sum_{i=1}^{k} \alpha_i(t).\, F_i \tag{7}$$

We call 'MacNeal projection base' [6] the following base:

$$V = [\Phi, \Psi] = [\varphi_1, \varphi_2, \ldots, \varphi_p, \psi_1, \psi_2, \ldots, \psi_k] \tag{8}$$

composed of p eigen modes of the linear structure and additional vectors ψ_i.
ψ_i is called a static mode and corresponds to the vector of the static displacements of the structure under load F_i. Thus, ψ_i can be written as :

$$\psi_i = K^{-1}.F_i \tag{9}$$

This projection base has been previously used in substructuring [6]. It retains the advantages of the base described in Section III.1.1. But, by virtue of the ψ_i vectors, the exact structural static flexibility is now represented. The only criterion for determining the number of vectors of the base is in this case to take the first p normal modes (plus the static modes) such that:

$$\omega_{p+1} \geq \alpha.\omega_{max} \quad \text{with} \quad \alpha = \sqrt{2} \tag{10}$$

III.2 - Projection base for a non-linear structure : (especially with local impact/friction non-linearities)
The previous bases proposed in case of linear systems can of course be used in the case of non-linear systems. Indeed, the Vibic [1] or Gerboise [2] computer codes dealing with impact and friction systems use the modal base of the free linear system (neglecting support non-linearities). It can be noted that this base is not always an optimum choice, mainly for multi-supported tubes whose response with impact on the loose supports is very different from the free vibration modes of the structure. In this case, the use of the linear modal base requires a large number of modes to get an accurate solution. Some other possible bases adapted to impact/friction conditions are now reviewed.

III.2.1 - Tangent modal base : To simulate impact/friction vibrations of a structure, one has to solve a non-linear dynamic problem. The choice of an accurate projection base is more difficult because the stiffness of the system changes with time. For a generic non-linear system, it has been shown [8] that the best projection base is the modal base of the tangent linearized problem. Nevertheless, it is somewhat arduous to compute it again, at each integration step. For a structure with impact vibrations, one can consider two separate cases depending whether the structure is free at the support or in contact with the support. These two phases correspond to two different modal bases with free or constrained limit conditions at the support. A possible choice for the projection base is then to build a mixed modal base (see Figure 1) with free and constrained modes at supports, and use it throughout the computation. The algorithm implemented in the Aster code allows the use of such a projection base.

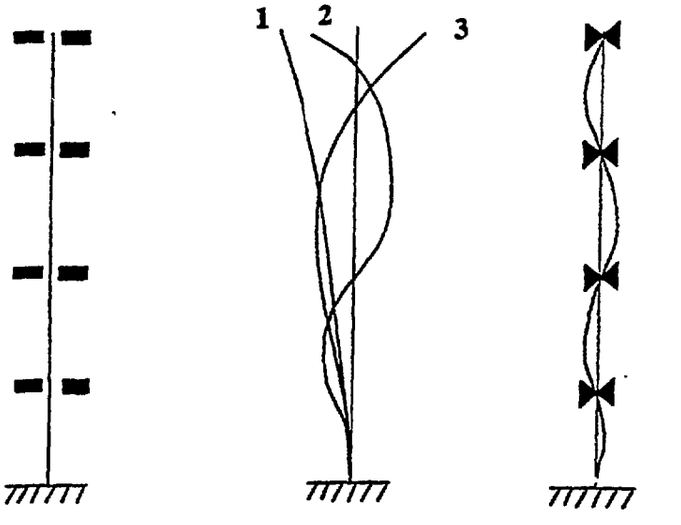

Fig. 1 - Mixed modal base for multi-supported tubes

III.2.2 - Craig-Bampton projection base : An other projection base used in substructuring can prove to be very effective for the simulation of impact/friction vibrations. This is what we call the 'Craig-Bampton base' [7]. It is composed of a modal base with constrained (pinned) conditions at the supports completed with static constraint modes. Those constraint modes are obtained by imposing a unit displacement at one support, the other support conditions staying constrained (pinned) (see Fig. 2 below). It is easy to see that, for narrow gap conditions, the pinned modal base is one of the most accurate representations of the actual vibration modes of the tube with impact. The static modes help to represent tube displacements at supports.

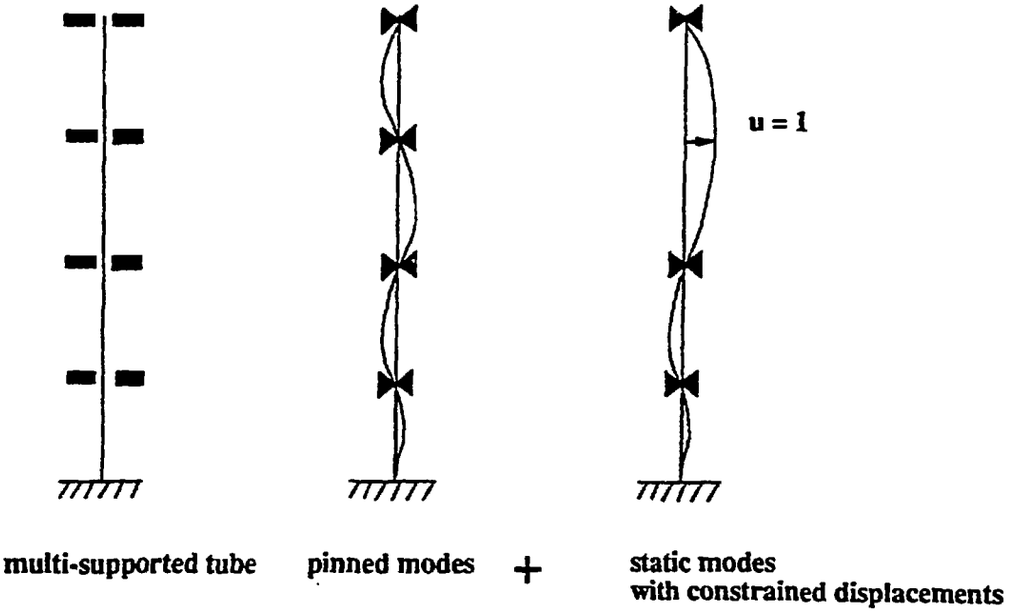

Fig. 2 - Craig-Bampton base for multi-supported tubes

To illustrate the different possible choices and the results obtained, consider a numerical examplre consisting in a clamped-free tube excited by a shaker. The system geometry is detailed in Figure 3

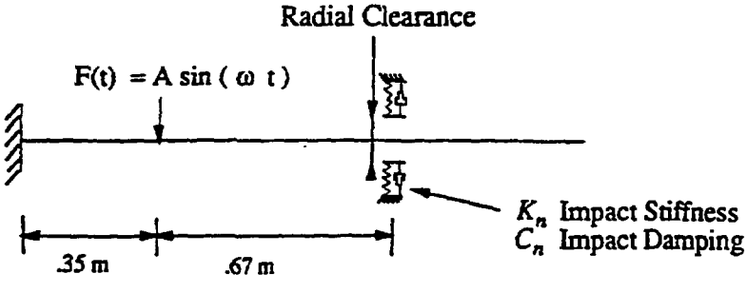

Structural parameters :

- tube length	L = 1.5 m
- outside diameter	D_e= 10.01 mm
- inside diameter	D_i = 9.0 mm
- Young's modulus	E = 2. 10^{11} Nm^{-2}
- density	ρ = 7800 $kg.m^{-3}$
- modal damping :	ξ = 0.5 %

Support parameters :

- clearance	c = 1.0 mm
- impact stiffness	K_n = 1. 10^7 N/m
- impact damping	C_n = 0 Ns/m

Excitation force is given by :

- frequency :	f = 6.0 Hz
- amplitude :	A = 2.0 N

Fig. 3 - Geometry of straight tube shaker test facility

Figure 4 compares convergence of the RMS impact force versus the number of vectors for the three base tested. It shows that all these bases converge finally towards the same value. The 'Craig-

Bampton base' appears to get a faster convergence than the usual modal base. The mixed or tangent bases which should bring the best results gives here the poorest convergence rate because we used half vectors of each base (which leads to a rather ill-conditionned projection base). The advantage of the 'Craig-Bampton base' which is here rather little would have been more important if we had choosen a multi-suppported test.

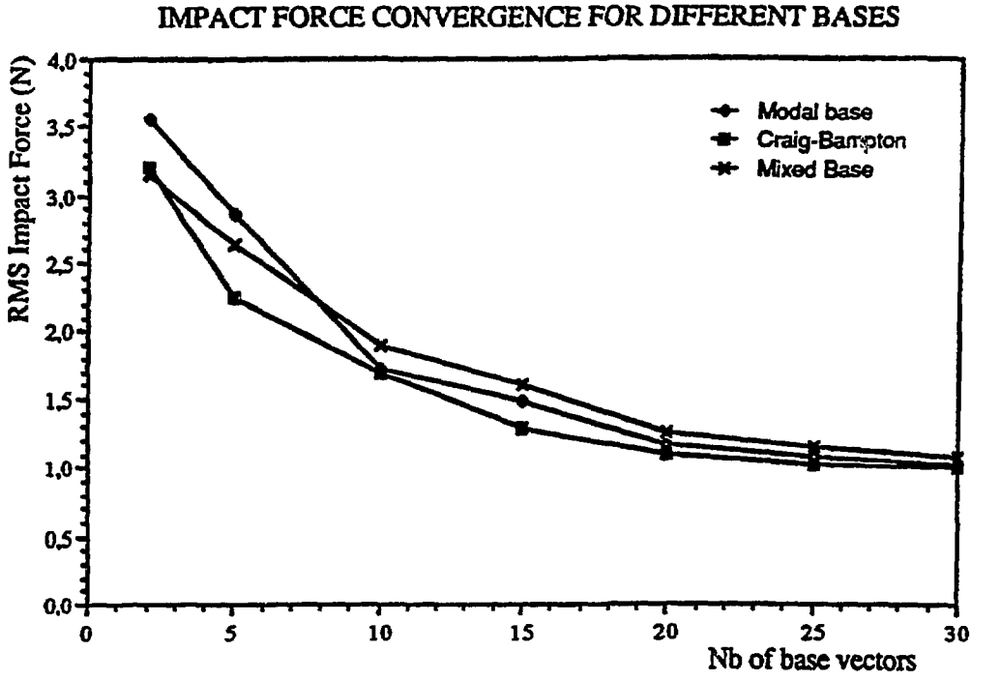

Fig. 4 - Convergence of the RMS impact force for different projection bases

VI - LOCAL IMPACT/FRICTION NON-LINEARITY MODELS

The algorithm developed in the Aster code to solve Problem (2) can take into account local impact/friction non-linearities between some points of the structure and elastic obstacles (supports, anti-vibration bars, guiding plate supports etc). The impact and friction force models, implemented here, use an explicit expression of normal and tangential reaction which is fully described in [5]. The normal impact force at one point, f_n, can be expressed knowing the normal distance to the obstacle and the normal velocity as (see Figure 5) :

$$f_n = -K_n . d_n - C_n . v_n \quad \text{if } d_n < 0, \quad \text{and} \quad f_n = 0 \quad \text{if } d_n \geq 0 \tag{11}$$

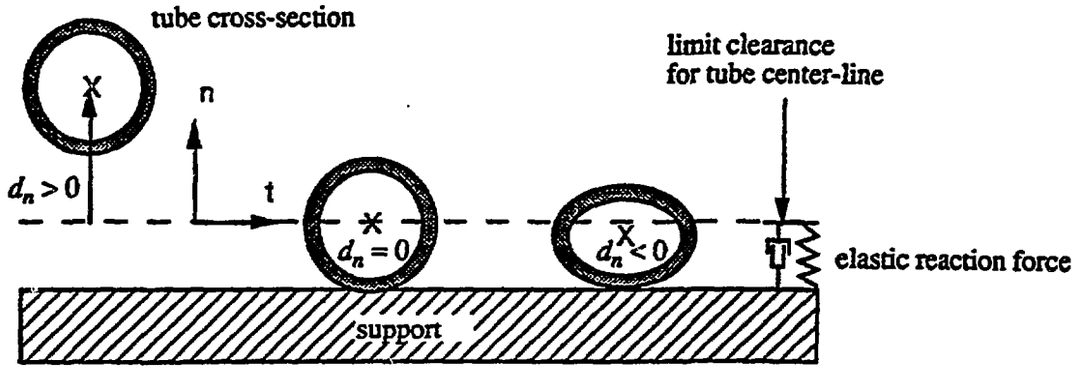

Fig. 5 - Normal impact force model

During contact periods, the tangential reaction force, $\vec{f}_t$ uses the Coulomb friction model, with a special treatment of adherence phases modeled by a linear spring with damping (see Figure 6). This yields

$$\vec{f}_t = -\mu . f_n . \frac{\vec{v}_t}{\|\vec{v}_d\|} \quad \text{if } \vec{v}_t \neq 0 \ , \quad \text{else} \quad \vec{f}_t = \vec{f}_t^{\,0} - K_t . (\vec{d}_t - \vec{d}_t^{\,0}) - C_t . \vec{v}_t \tag{12}$$

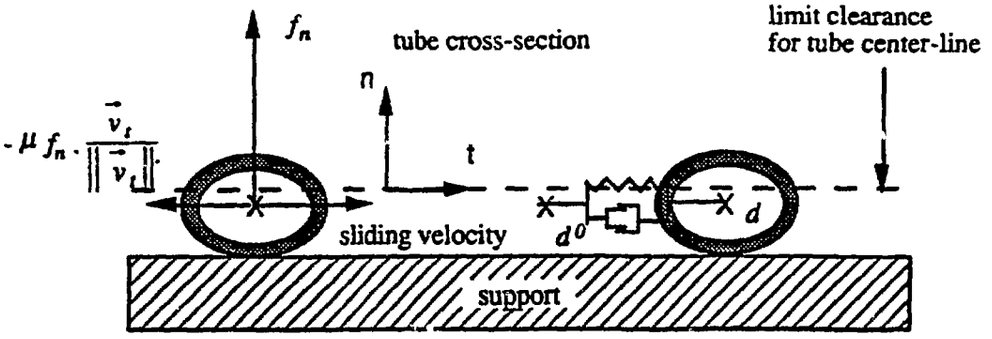

Fig. 6 - Tangential impact force model during contact periods

V - NUMERICAL INTEGRATION OF THE DYNAMIC SYSTEM

The reduced dynamic problem (2) is formulated as:

$$m . \ddot{q} + c . \dot{q} + k . q = r(t) + g\,(q, \dot{q}) \tag{13}$$

This matricial differential system is integrated by a simple explicit integration scheme, i.e. the modified Euler scheme.

$$\begin{aligned} &\text{knowing } \dot{q}_t \ , q_t \ , \text{ compute} \\ &\ddot{q}_t = m^{-1} . \left(r(t) + g\,(q_t, \dot{q}_t) - c . \dot{q}_t - k . q_t \right) \\ &\dot{q}_{t+dt} = \dot{q}_t + dt . \ddot{q}_t \\ &q_{t+dt} = q_t + dt . q_{t+dt} \end{aligned} \tag{14}$$

This explicit integration scheme has been chosen for its simplicity and its satisfactory results even when compared to other higher-order schemes (Runge-Kutta or De-Vogelaere). Moreover, it is well adapted to deal with an adaptive time step. As in any explicit scheme, a very short integration time step is needed. To obtain a high accuracy a time step equal to 1 to 5% of the shortest eigenperiod of the system is needed.

VI - NUMERICAL EXAMPLES

In order to validate the implementation of the numerical algorithm, numerical examples of a single and also multi-supported tube with impact vibrations have been selected in an article by Sauvé-Teper [3]. This section gives a comparison of the results by Sauvé with the Aster code computation for these two configurations.

VI.1 Tube with single support interaction

The model consists of a tube fully clamped at both ends, with a loose support at its center limiting the amplitude of the displacements. A periodic excitation is applied at 4 points along the structure.

The geometry and structure characteristics are recalled in Figure 7.

The Aster computation has been performed using a simple modal base of 10 modes. Time histories for the tube displacements and impact forces obtained with the Aster code are presented in Figure 8a and 8b respectively. A good agreement with Reference [3] can be noted. The RMS impact force and the mean contact duration have also been computed and are listed in Table 1.

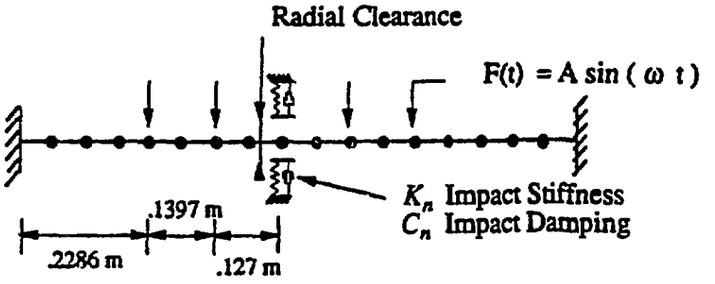

Structural parameters:

- tube length $L = 0.9906$ m
- outside diameter $De = 15.375$ mm
- inside diameter $Di = 9.525$ mm
- Young's modulus $E = 2.10^{11}$ Nm^{-2}
- density $\rho = 7740$ $kg.m^{-3}$
- structural damping $C = \beta M + \gamma K$
  $\beta = 4.$
  $\gamma = 5. 10^{-6}$

Support parameters :

- clearance $c = 0.127$ mm
- impact stiffness $K_n = 1.75\ 10^{6}$ N/m
- impact damping $C_n = 0.2$ Ns/m

Excitation force is given by :

- frequency : $f = 84.0$ Hz
- amplitude : $A = 2.85$ N

Fig. 7 - Single support tube test geometry

Impact Force (simple mean)	4.26 N
RMS Impact Force	0.71 N
Contact Duration (simple mean)	1.30 ms

Table 1 - Predicted mean results for the single support tube

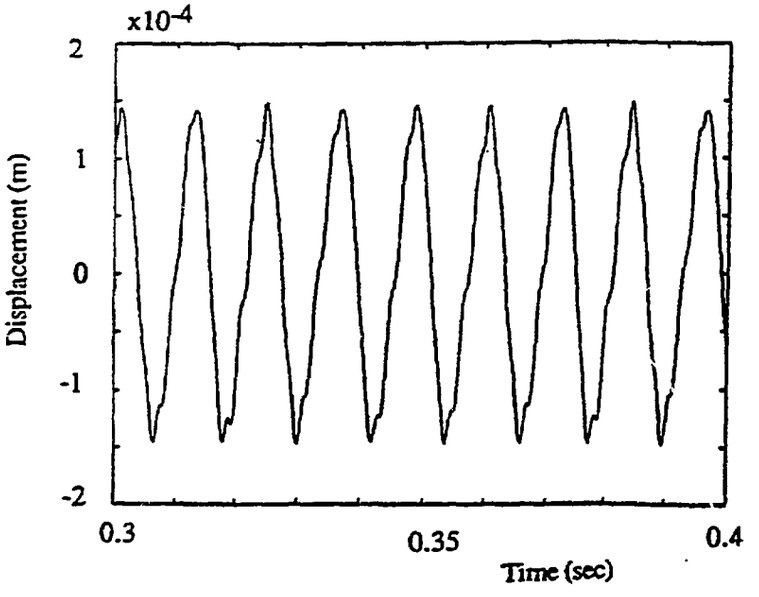

Fig. 8a - Tube displacement time history at loose support

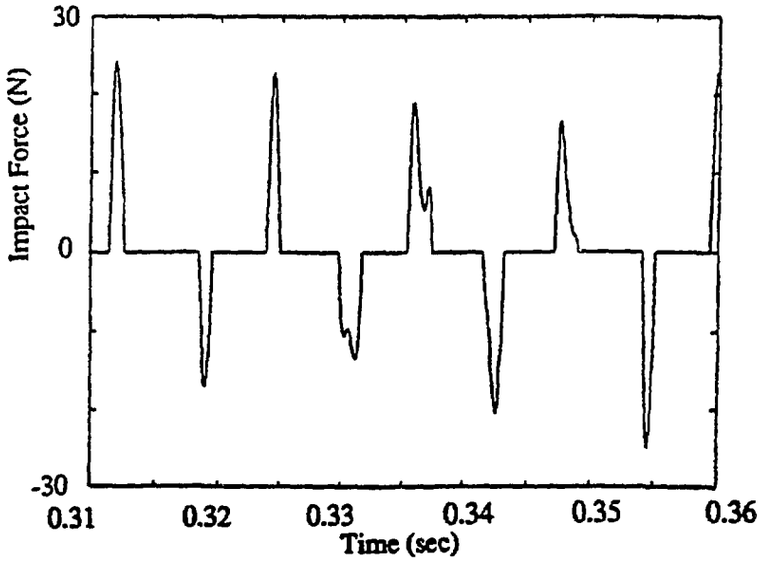

Fig. 8b - Impact force time history at loose support

V.2 A multi-supported tube test:

The model consists in a tube fully clamped at one end free at the other end, with four regularly spaced supports. The tube is subjected to a flow excitation with alternative phase on each span. A parametric study of the RMS impact force at support 4 with different clearance values was conducted.

The geometry and physical properties of the structure are presented in Figure 9:

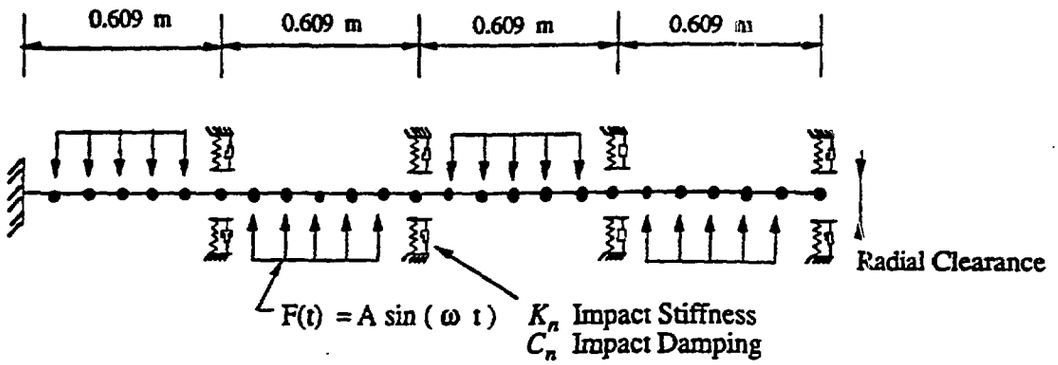

Structural parameters :

- length L = 2.436 m
- outside diameter De= 15.9 mm
- inside diameter Di = 13.6 mm
- Young modulus $E = 2.07\ 10^{11}\ Nm^{-2}$
- density $\rho = 7870\ kg.m^{-3}$
- structural damping $C = \beta M + \gamma K$, $\beta = 0.1526$, $\gamma = 1.79\ 10^{-5}$

Supports parameters :

- identical clearances c = 0.001 mm, 0.2 mm, 0.406 mm, 0.6 mm
- impact stiffness $K_n = 1.75\ 10^6 N/m$
- impact damping $C_n = 0.28\ Ns/m$

Excitation force is defined by :

- frequency : f = 40.0 Hz
- amplitude : A = 41.38 N/m

Fig. 9 - Multi-supported tube test

Times histories of the tube displacement and impact forces have been computed by Aster with a simple modal base of 30 modes. Computational results refering to the 0.406 mm clearance configuration, are shown in Figure 10. A good agreement with Reference [3] can be noted. On the

other hand, the RMS impact force at support 4 as function of clearance can be successfully compared with other computer codes results. This comparison is presented in Table 2.

RMS Impact Force at support 4	clearance 0.001 mm	clearance 0.2 mm	clearance 0.406 mm	clearance 0.6 mm
Vibic	10 N	16.6 N	22.5 N	28.5
H3DMAP	9.4 N	20 N	25.3 N	30 N
Aster	10 N	17 N	23.1 N	27.8 N

Table 2 - Comparison of RMS impact force at support 4

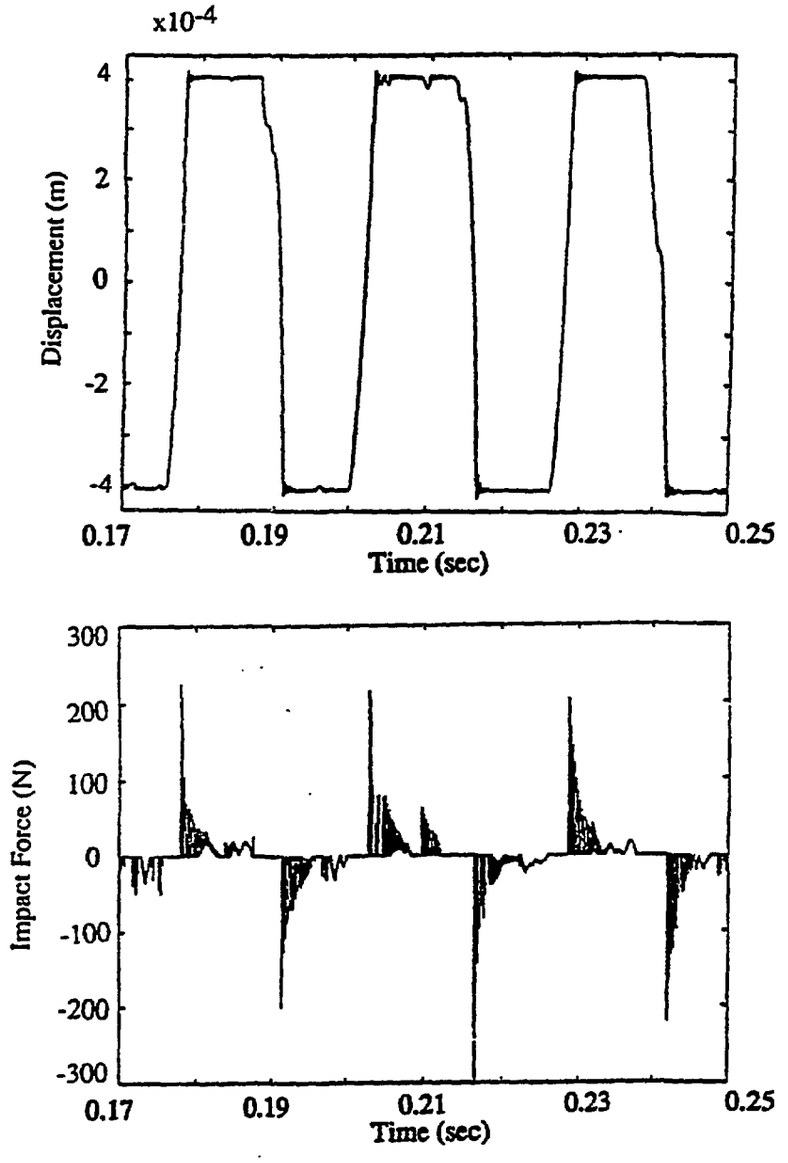

Fig. 10 - Displacement and impact force time histories at support 4

The previous two numerical examples show that, for single or multi-supported tubes, the algorithm implemented is able to accurately compute the mean displacements and impact forces. It has been positively compared with codes using modal superposition such as Vibic or using direct integration and Newton iterations such as H3DMAP.

The next section covers validation of the numerical model on an industrial shaker test facility, and checking the degree of confidence of numerical simulation versus experimental measurements.

VII - EXPERIMENTAL VALIDATION

The experimental validation proposed here is based on test results obtained on a U-bend shaker test model [9] and [10]. As well as the present numerical simulation, they are a part of a joint multi-party research program. They are therefore confidential, and only relative values or curves with arbitrary scales can be provided in this section.

VII.1 - Experimental Apparatus

Figure 11 is a schematic representation of the shaker test facility, which provided the experimental data used for the proposed validation. This facility is fully detailed in [9] and [10].

The mechanical system chosen for the numerical simulation with ASTER consists in the curved U-bend tube with four anti vibration bar (AVB) locations [6]. The tube has 1.02m straight leg sections that are fixed at the lower end of the tube (locations SE and SE' on Fig. 11). The top support plate of the steam generator is simulated in the tests by four steel knife-edge strips positionned 90° appart around the tube circumference (locations SD and SD'). The four AVB locations along the tube are named C1, C2, C3, and C4. Supports with small clearances exist at locations C1, C2 and C4. This clearance is equal to Gs. An inactive support with large gap is positionned at C3. The gap for this support Gl is fifteen times greater than Gs. The radius of the U-bend tube is 1.5m, the external and internal diameters of the tube are respectively equal to 17.5 10^{-3} m and 15.4 10^{-3} m. The tube is filled with water and pressurized to 8.273 10^{6} Pa. The U-bend region of the tube is vibrated in the out of plane and in plane directions by electromagnetic shakers referred as Eo and Ei on Fig. 11. The shaker located at the apex of the tube, i.e. Eo, provides sinusoïdal excitation in the out-of-plane direction. The other one, Ei, is oriented in the radial in-plane direction and delivers a random excitation.

The available data for a comparison of experimental results with numerical simulations are limited to time histories at support C2 and C3, and work rate estimated by the experimentators at these support locations.

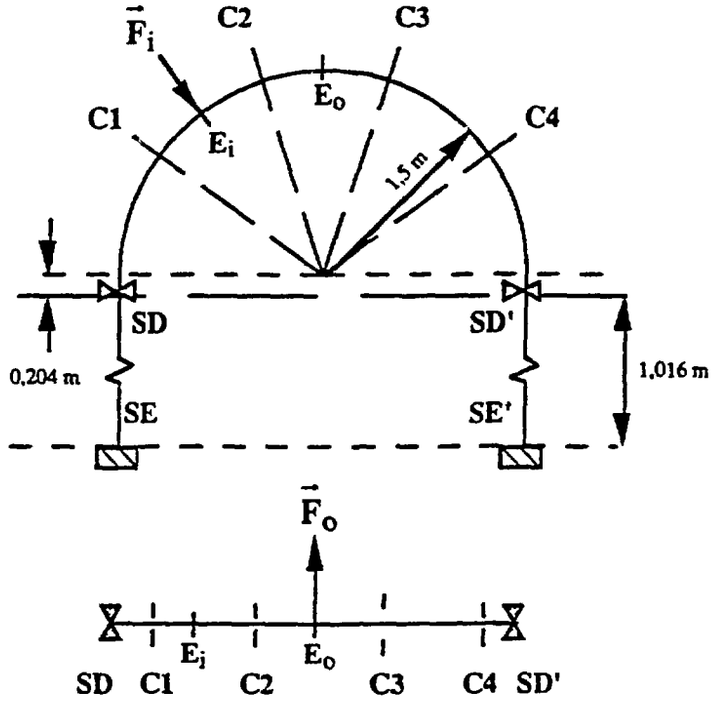

Fig. 11 : Westinghouse shaker test facility

VII.2 - ASTER Simulation Characteristics

For the numerical simulation with ASTER, the support conditions are assumed to be :

- locations SE and SE' : clamped
- locations SD and SD' : pinned
- locations C1, C2, C4 : support with small gap Gs
- location C3 : support with large gap Gl.

The tube is defined with 178 finite elements, 30 elements for each straight leg section, 8 elements for the straight part comprised between the top support plate and the U-bend beginning, and 102 elements in the U-bend itself.

The modal base taken into account for the numerical simulation corresponds to a configuration with supports C1, C2, C3 and C4 totally released.

The sinusoïdal out of plane force can be defined by the following equation :

$$Fo = A \sin(2\pi f_0 t) \quad (15)$$

and for the tests simulated here, the driving frequency f_0 of the sinusoïdal excitation was equal to 15.4 Hz. The random in plane excitation is characterized by the power spectral density of the excitation signal S_{ir}.

The nonlinear dynamic response of the tube is computed for two cases corresponding to different excitation configurations :

- case 1 : $Fo = A \sin(2\pi f_0 t)$, $Fi = 0$
- case 2 : $Fo = A \sin(2\pi f_0 t)$, Fi characterized by S_{ir}

For the present simulations , a single set of parameters has been chosen to describe the non linear interaction between the tube and its supports and is kept constant for all the excitations.

This set of parameters is composed of the tube damping for each mode, the normal and tangential stiffnesses of the loose supports, the damping of the support in the normal and tangential directions, the friction coefficient.

VII.3 - Numerical Results / Experimental Data Comparison

As a first step, the experimental time histories of the signals obtained on supports C2 and C3 are compared to the simulation results. The final goal of the numerical/experimental result comparison is to be able to evaluate the accuracy of work rate prediction with the computer code.

In the U-bend shaker tests , significant work rate has been measured at support C2 and C3 even for a supposed purely out-of-plane excitation (case 1). In the idealized numerical simulation of a tube excited by a solely out-of-plane excitation, such a wear phenomenon cannot be obtained. This assessment yields to a second non-idealized representation of the mechanical system, considering a slight angular deviation of shaker Eo with respect to the pure out-of-plane direction. In this second simulation, the angular deviation chosen generates an in-plane component for the sinusoïdal excitation, whose amplitude is less than 10 percent of the out-of-plane one. Anyway, such an approach will make it possible to estimate the sensitivity of the system to a slight perturbation of its geometrical characteristics. This representation is not the only one that could have been chosen to create a tangential displacement of the tube at its support location. Another solution could have been to consider twisted positions of the tube within its supports. In the present paper, we will focus our analysis on the perturbation due to the excitation force direction.

A typical example of a measured and computed time history for the normal impact force and tube displacement is provided in Figures 12 and 13. In Figure 12, for each support location, two impact force signal are presented, corresponding respectively to the impacts measured on the front AVB and on the back AVB. The tube displacement between front and back AVBs is shown also. Figure 13 presents the normal impact forces at C2 location obtained for case 2 excitation with an angular deviation for shaker Eo. It can be noted that the computed imapct force in this Figure is alternatively positive and negative. This must be interpreted as follows : a positive impact force corresponds to a contact between the tube and the front AVB ; a negative impact force denotes a contact between the tube and the back AVB. The expanded time scale enables to appreciate the good accordance between experiment and computation for the shape of the impacts, the amplitude of the impact force, the mean contact duration. Tables 3 and 4 provide the relative values for work rate at supports C2 and C3, taking account or not the angular deviation at Eo, for respectively the excitations defined in case 1 and 2 These relative values are obtained from measured and computed work rates with the formula :

$$\varepsilon_{\dot{W}} = (\dot{W}_c - \dot{W}_m) / \dot{W}_c \quad (16)$$

where $\varepsilon_{\dot{W}}$ is the relative error on work rate, $\dot{W}_c$ is the computed work rate in the ASTER simulation, $\dot{W}_m$ is the measured work rate in the Westinghouse experiment

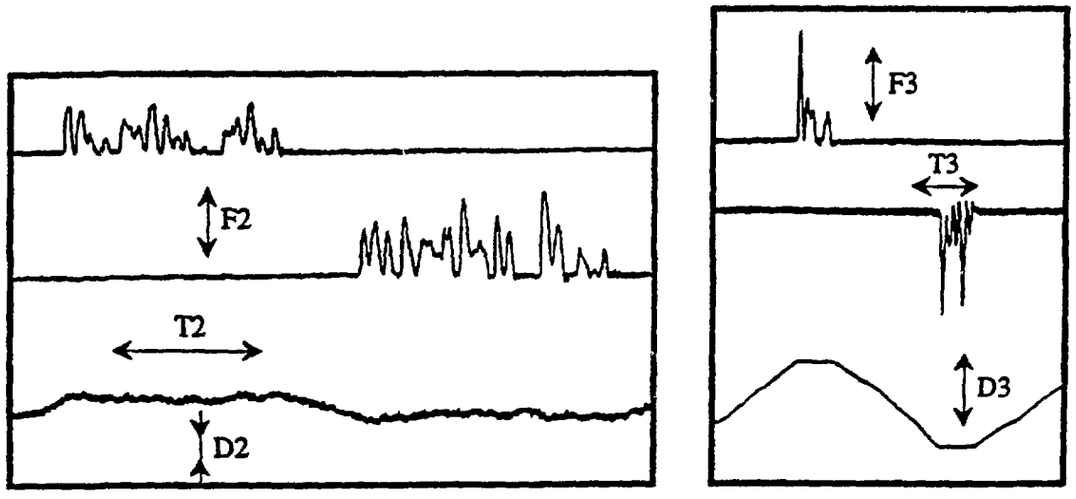

Support C2 Support C3

Fig. 12 : Measured time histories for normal impact force and displacement at supports C2 and C3 (case 2)

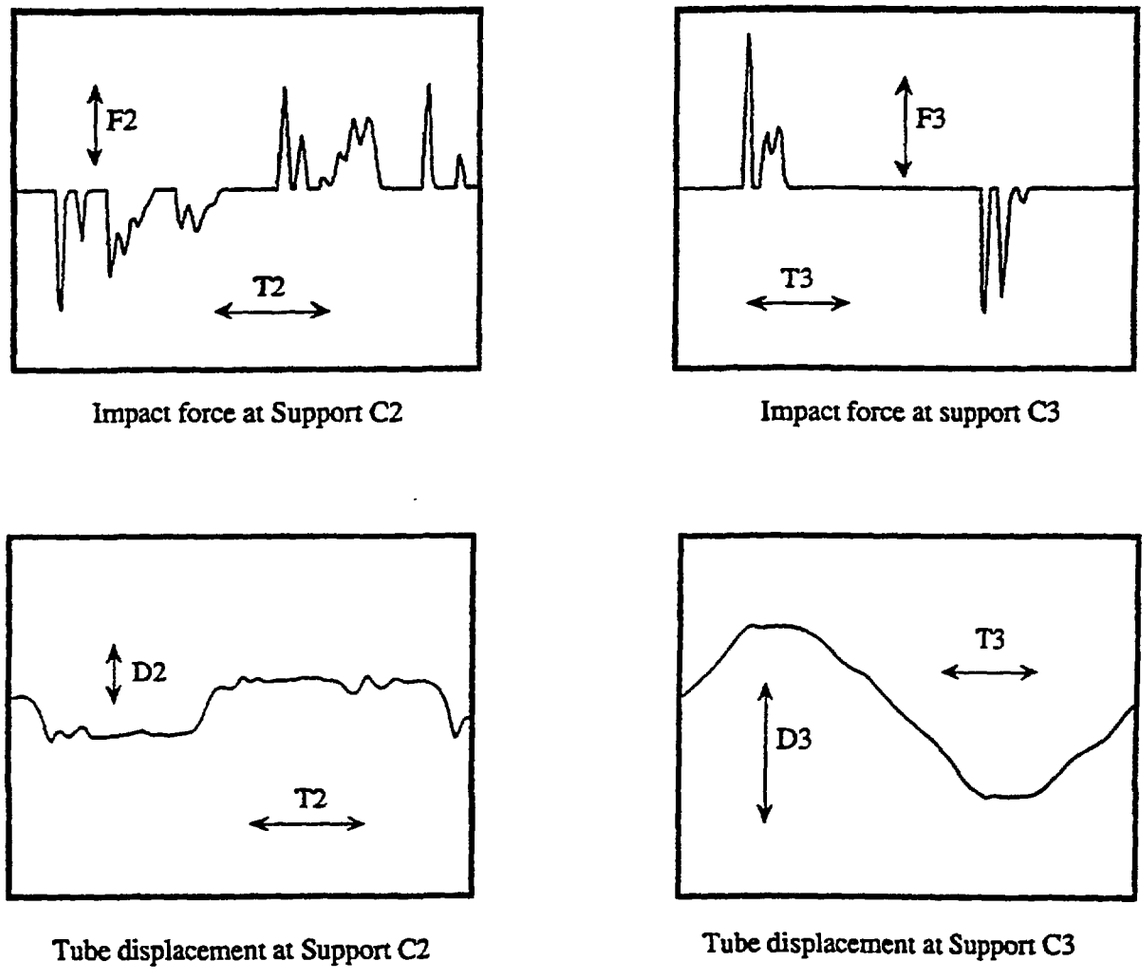

Impact force at Support C2 Impact force at support C3

Tube displacement at Support C2 Tube displacement at Support C3

Fig. 13 : Computed time histories for normal impact force and displacement at supports C2 and C3 (case 2)

	Relative work rate without angular deviation modelization	Relative work rate with angular deviation modelization
Support C2	$-6.5\ 10^6$	-10.0
Support C3	$-1.0\ 10^7$	-24.2

Table 3 : Relative error on work rate for excitation defined in case 1

	Relative work rate without angular deviation modelization	Relative work rate with angular deviation modelization
Support C2	0.35	0.36
Support C3	0.036	0.36

Table 4 : Relative error on work rate for excitation defined in case 2

As expected, it appears that for case 1, potential for wear cannot be modeled with a solely out of plane excitation. The very strongly negative values obtained in Table 3 for the relative error without angular deviation modelization, are particularly significant of a total incapability to reproduce, with an idealized modelization, the physical phenomena which generate work rate for this experiment. Let us analyze the relative error values related to case 1 with angular deviation modelization. These values remain negative, but it can be noted that the order of magnitude for the relative errors is considerably changed. It means that, even still under-estimated by a factor of 10 or 20 according to the support considered, a significant potential for wear has been obtained. We will not claim the proposed angular deviation modelization to be *the* physical mechanism that produces work rate in the U-bend shaker experiment . However, such an approach, taking into account a very slight perturbation for one of the input simulation parameters, shows that the computation results may be very sensitive to the input data. Examine now, results provided in Table 4. We can easily conclude that as soon as in-plane random excitation is large enough to generate a significant tangential motion, the effect of the angular deviation modelization becomes negligible. We can also note that such an excitation configuration as case 2, is accurately represented by the computer code with an idealized modelization, since random excitation governs the in-plane motion for the vibrating tube. This corroborates the very good accordance between the computed and experimental time histories in Figures 12 and 13.

CONCLUSION

The problem of tube fretting-wear caused by flow induced excitations requires a wide range of studies from the fluid/structure excitation mechanisms, the impact/friction dynamics to the wear analysis. This paper has presented a numerical method for evaluating transient displacements and impact forces of a vibrating structure with loose supports. This algorithm has been incorporated in the DFR general structural computer code Aster. Numerical examples treated by previous authors have been selected to validate the algorithm. A good agreement has been obtained. A comparison with experimental measurements on a U-bend tube show that impact forces and displacements are reproduced by the code with a relatively good accuracy. Moreover, wear rates can be estimated with a less than 35% error, which can be considered has a good result. Further works have to be done to get a complete tool helping us to understand and design components experiencing flow-induced vibration with impact-friction. Different fluid excitation descriptions will have to be incorporated in the

numerical code. A program relating computed wear rate to a worn volume or to a tube wall thining has also to be developed.

ACKOWLEDGMENTS

The experimental data and simulation results of Section VII are part of a four-party joint research program sponsored by Framatome, Westinghouse, Commissariat à l'Energie Atomique (CEA) and Electricité de France (EDF). The experimental data were obtained on the Westinghouse U-bend shaker experiment by Dr. H.J. Connors and F.A. Kramer.

REFERENCES

[1] P.L. Ko and R.J. Rogers, *Analytical and experimental studies of tube/support interaction in multi-span heat exchanger tubes*, Nuclear Engineering and Design, Vol. 65 1981, pp399-409

[2] F. Axisa, A. Paurobally and A. Remond, *Predictive analyses of flow induced vibration and fretting wear in steam generator tubes*, International Conference on Pressure Vessel Technology , Nuclear codes and Standards, Seoul 89

[3] R.G. Sauvé and W.W. Teper, *Impact simulation of process equipment tubes and support plates- A numerical algorithm* , Journal of Pressure Vessel Technology, Feb.87, Vol. 109, pp70-79

[4] N.J. Fisher, M.J. Olesen R.J. Rogers and P.L. Ko, *Simulation of tube to support dynamic interaction in heat exchanger equipment*, ASME 88 Annual Winter Meeting, International Symposium on Flow Induced Vibration and Noise

[5] J. Antunes and F. Axisa *et al., Coulomb friction modelling in numerical simulations of vibration and wear work rate of multispan tube bundles*, Journal of Fluids and Structures (1990) 4, pp287-304

[6] R.H. MacNeal, *A hybrid method for component modes synthesis*, Journal of Computers Vol. 1, No. 4, December 1971, p581-601

[7] R. Roy Jr. and Craig C. Bampton, *Coupling of substructures for dynamic analyses*, AIAA Journal Vol. 6, No. 7, July 1968

[8] R.E. Nickel, *Non-linear dynamics by mode superposition*, Computer Methods in Applied Mechanics and Engineering, Vol 7, pp107-129, 1976

[9] France, E.R., Connors, H.J.,1991, *"Simulation of Flow Induced Vibration Characteristics of a Steam Generator U-Tube"*, Flow Induced Vibrations, International Conference, 20-22 May 1991, Brighton, England, Paper C416/020, pp. 33-44

[10] Connors, H. J., Kramer, F. A., 1991, *"U-Bend Shaker Test Investigation of Tube/AVB Wear Potential"*, Flow Induced Vibrations, International Conference, 20-22 May 1991, Brighton, England, Paper C416/014, pp. 57-68